

Structure of InAs/AlSb/InAs resonant tunneling diode interfaces

B. Z. Nosho^{a)} and W. H. Weinberg

Center for Quantized Electronic Structures and Department of Chemical Engineering,
University of California, Santa Barbara, California 93106

J. J. Zinck

HRL Laboratories, Malibu, California 90265

B. V. Shanabrook, B. R. Bennett, and L. J. Whitman^{b)}

Naval Research Laboratory, Washington, DC 20375

(Received 21 January 1998; accepted 20 May 1998)

We have used *in situ* plan-view scanning tunneling microscopy to study the surfaces and interfaces within an InAs/AlSb/InAs resonant tunneling diodelike structure grown by molecular beam epitaxy. The nanometer and atomic-scale morphologies of the surfaces have been characterized following a number of different growth procedures. When InAs(001)-(2×4) is exposed to Sb₂ a bilayer surface is produced, with 1 monolayer (ML) deep (3 Å) vacancy islands covering approximately 25% of the surface. Both layers exhibit a (1×3)-like reconstruction characteristic of an InSb-like surface terminated with >1 ML Sb, indicating that there is a significant amount of Sb on the surface. When 5 ML of AlSb is deposited on an Sb-terminated InAs surface, the number of layers observed on each terrace increases to three. Growth of an additional 22 ML of InAs onto the AlSb layer, followed by a 30 s interrupt under Sb₂, further increases the number of surface layers observed. The root-mean-square roughness is found to increase at each subsequent interface; however, on all the surfaces the roughness is ≤2 Å. The surface roughness is attributed to a combination of factors, including reconstruction-related stoichiometry differences, kinetically limited diffusion during growth, and lattice-mismatch strain. Possible methods to reduce the roughness are discussed.

© 1998 American Vacuum Society. [S0734-211X(98)08304-8]

I. INTRODUCTION

A wide range of band alignments are possible between the nearly lattice matched “6.1 Å” family of III–V semiconductors, InAs, GaSb, and AlSb, allowing a variety of novel quantum well and superlattice-based electronic devices to be fabricated from these materials, including infrared detectors, infrared lasers, and high-speed oscillators. For example, resonant tunneling diodes (RTDs) with switching speeds approaching terahertz frequencies can be constructed using thin AlSb layers [5–10 monolayers (ML)] as tunneling barriers between InAs- and GaSb-based layers.^{1–3} The properties of these devices are highly dependent on the barrier thickness,⁴ as expected given that transport across the barrier depends exponentially on thickness. RTD performance is also expected to be sensitive to atomic-scale variations in the morphology of the interfaces,⁵ including fluctuations in film thickness and composition caused by diffusion and/or intermixing during growth. Characterizing, understanding, and ultimately controlling the atomic-scale structure of the interfaces within RTDs will be essential to reproducing device characteristics within the tight tolerances required for integration into high-speed circuits.

Many recent studies have focused on determining the best method for making interfaces between different 6.1 Å layers using molecular beam epitaxy (MBE).^{6–10} For example, two different types of interfacial bonds can be formed during the

deposition of AlSb on InAs, either AlAs like or InSb like, depending on the III–V deposition sequence. It has been found both experimentally^{11–14} and theoretically¹⁵ that InSb-like interfaces are generally more abrupt than those with AlAs-like bonds. For this reason, among others, AlSb-based tunneling devices are usually fabricated with InSb-like interfaces. One approach for preparing an AlSb-on-InAs interface with InSb bonds using MBE would be to: terminate the In and As₂ fluxes; then start the Sb₂ flux, exposing the surface to just Sb₂ for a brief time (typically 5–30 s, i.e., a “growth interrupt”); and then start the deposition of Al to begin AlSb growth. It has been reported that during the Sb₂ exposure the As on the surface is largely replaced by Sb.¹⁶ One possible way to reduce such an anion exchange might be to use migration enhanced epitaxy (MEE) to form the interface, depositing the individual III and V elements sequentially. For example, to deposit AlSb on InAs with an InSb-like interface one can first deposit an additional ML of In (with no As₂ flux), then briefly expose the surface to Sb₂ (with no In or Al flux). After the desired amount of Sb is deposited, AlSb growth is begun. In principle, this procedure should be less conducive to anion exchange, enabling more abrupt, consistent interfaces to be formed.

In this article we describe our scanning tunneling microscopy (STM) study of the surfaces and interfaces formed during the growth of InAs/AlSb/InAs RTD-like structures, focusing on InSb-like interfaces prepared by MEE. InAs substrates were used, rather than InAs buffer layers grown on GaAs substrates, in order to eliminate any artifacts that

^{a)}Electronic mail: brett@engineering.ucsb.edu

^{b)}Electronic mail: Lloyd.Whitman@nrl.navy.mil

might arise as a consequence of the greater roughness of InAs surfaces grown on GaAs. We have examined the effects of various growth procedures on the apparent anion exchange reaction, and the resulting surface morphology of subsequently deposited films. Based on the analysis of our results, we discuss possible routes for improving the quality and consistency of the interfaces in these structures.

II. EXPERIMENT

The experiments were performed at the Naval Research Laboratory in an interconnected, multichamber ultrahigh vacuum facility that includes a III–V MBE chamber equipped with reflection high-energy electron diffraction (RHEED) and a surface analysis chamber equipped with a STM.¹⁷ All films were grown not intentionally doped using “cracked” As₂ and Sb₂ sources on undoped InAs(001) wafers. The growth rates were monitored by RHEED oscillations. After oxide removal, all growths were begun with a $\sim 0.5 \mu\text{m}$ thick buffer layer of InAs grown with a 5:1 beam equivalent pressure (BEP) ratio of As-to-In at 1 ML/s with 30 s interrupts under As₂ every 90 s. The growth temperature was kept 10 °C below the temperature at which the (2 \times 4)–to–(4 \times 2) transition occurs during InAs growth (estimated to be 490 °C).¹⁸ At the end of the buffer layer growth, the In was shuttered and a 10 min growth interrupt was performed (i.e., the samples were held at the growth temperature while reducing the As₂ flux), during which time the RHEED patterns progressed from a streaky (2 \times 4) to sharp diffraction spots along each streak. The samples were cooled approximately 100 °C after completion of the InAs buffer layer and prior to the growth of AlSb. In order to minimize unwanted deposition leaking from the shuttered sources, the sample surfaces were rotated away from the sources during this time. Once the temperature stabilized, the samples were rotated back to face the sources and all further growths were performed at the lower temperature.

Each image in our study can be considered to be a “snapshot” of the surface at some point during the growth of InAs/AlSb/InAs. A diagram of the structure grown and the surfaces and interfaces examined is displayed in Fig. 1. Note that although the interfaces were prepared sequentially as indicated, *a new sample was prepared from scratch for each interface studied* to eliminate any history effects associated with vacuum contamination, etc. Starting with the InAs buffer layer described above, the first interface was prepared using MEE, with 1 ML of In (1 s) followed by 2 s of Sb₂ at a BEP of $\sim 2.5 \times 10^{-6}$ Torr. This surface will henceforth be referred to as “the MEE-prepared surface.” On two different MEE-prepared surfaces, 5 ML of AlSb was then grown at 0.5 ML/s. One sample was immediately cooled after the AlSb deposition (with no Sb₂ flux), and the other was given a 5 min growth interrupt under Sb₂ for comparison. The final layer studied, 22 ML of InAs, was deposited on the interrupt-terminated AlSb layer, and given a 30 s interrupt under Sb₂ after growth. This surface would be the starting point for the second AlSb layer in a double-barrier resonant tunneling structure.

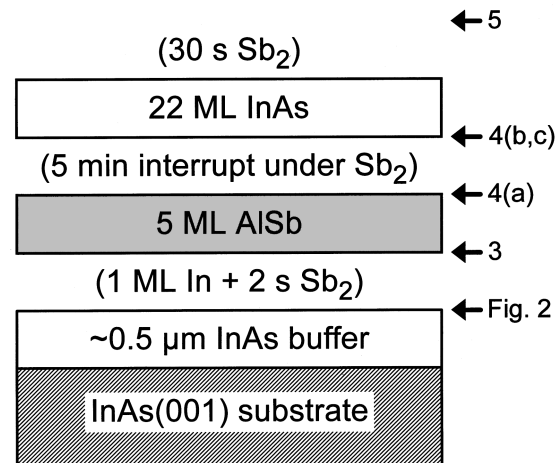


Fig. 1. Schematic diagram of the InAs/AlSb/InAs structure grown by MBE and studied with STM. Surfaces of interest begin with the InAs buffer layer and end at the surface on which a second AlSb barrier layer would be deposited. Notations in parentheses refer to surface treatments applied between the layers. Surfaces that are shown in Figs. 2–5 are indicated by the arrows.

After the completion of each growth, the sample was immediately removed from the MBE chamber and transferred to the STM chamber. The pressure in the transfer section was $< 5 \times 10^{-10}$ Torr, and the entire transfer procedure from the end of the growth until the sample was in the STM chamber typically took < 10 min. The samples were allowed to cool further for ~ 1 h in the STM chamber ($< 1 \times 10^{-10}$ Torr) before imaging. All STM images shown were acquired in constant-current mode with sample biases ranging from -1.5 to -3 V and tunneling currents between 50 pA and 0.5 nA.

III. RESULTS AND DISCUSSION

At the end of the 10 min interrupt the InAs(001) buffer layer is nearly ideal, composed of large (0.1–0.5 μm wide), atomically flat terraces separated by monolayer height (3 Å) steps, as shown in Fig. 2. There are essentially no islands (< 1 per $10 \mu\text{m}^2$), so the step density is simply determined by the surface orientation—approximately 0.05° from (001). Higher magnification images (not shown) reveal a well-ordered (2 \times 4) surface reconstruction similar in appearance to that observed on As-terminated GaAs(001), consistent with the sharp RHEED spots observed at the end of the growth procedure.

Terminating the InAs(001)-(2 \times 4) surface with InSb bonds via the MEE procedure described above (1 ML In+2 s Sb₂) dramatically changes the nanometer-scale surface structure, as shown in Fig. 3(a). The originally flat surface bifurcates into two levels, with 1 ML deep anisotropic vacancy islands (the lower level) covering 23% of the surface area. An analysis of the two-dimensional height–height autocorrelation function indicates that features on the surface are generally twice as long along $[\bar{1}10]$ than along $[110]$. A radial distribution analysis of the vacancy islands shows that they are randomly distributed across the surface

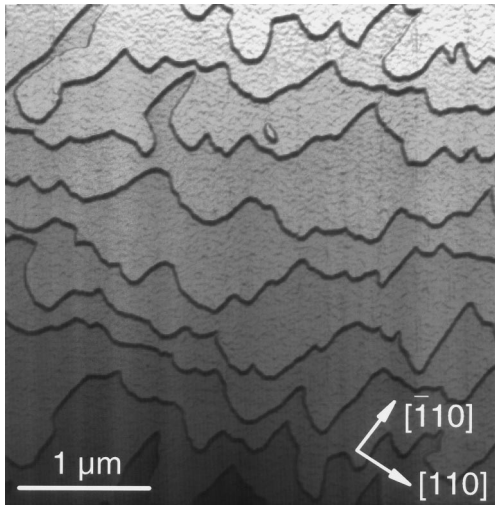


FIG. 2. $3.2\ \mu\text{m} \times 3.2\ \mu\text{m}$ STM image of the InAs(001)-(2 \times 4) buffer layer. Image is displayed as a three-dimensional (3D)-rendered gray scale with a very slight perspective. (This view enhances the 3.0 Å high step edges, which appear dark.)

at a density of $3.7 \times 10^{11}\ \text{cm}^{-2}$, with an average area of $42\ \text{nm}^2$ and separation of 17 nm. (These statistics are collated in Table I.) At higher magnification (not shown), a disordered (1 \times 3)-like reconstruction is observed, consistent with the corresponding streaky (1 \times 3) RHEED pattern. The reconstruction has a similar appearance to that observed on InSb,¹⁹ AlSb,²⁰ and GaSb.^{21,22} We believe the atomic-scale structure is similar to that proposed for GaSb(001)- $c(2 \times 6)$,^{22,23} which consists of a full 1 ML plane of Sb atoms terminated by $\frac{2}{3}$ ML of Sb in dimer rows [see Fig. 4(d)].

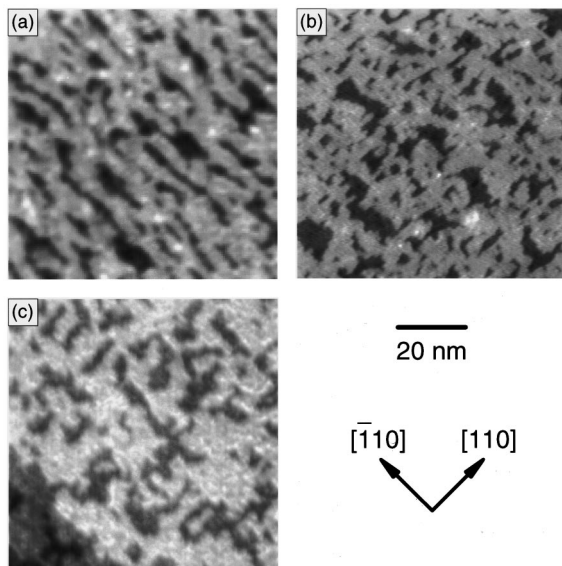


FIG. 3. Filled-state images, $80\ \text{nm} \times 80\ \text{nm}$, of an InAs(001)-(2 \times 4) surface exposed to: (a) 1 ML of In followed by 2 s of Sb_2 ; (b) 2 s of Sb_2 ; (c) 30 s of Sb_2 . In all three images the 3 Å deep vacancy islands cover approximately 25% of the surface.

TABLE I. Statistical comparison of the vacancy islands formed when InSb-like bonds are created on InAs(001) by exposing a (2 \times 4)-reconstructed surface to Sb_2 . Island density, average island area, and average island separation are indicated (along with the standard errors) for three different exposures.

Sample	Fraction on lower level	Density ($10^{11}\ \text{cm}^{-2}$)	Average area (nm^2)	Average separation (nm)
1MLIn+2 s Sb_2	23%	3.7 ± 0.5	42 ± 5	17
2 s Sb_2	24%	14.1 ± 0.8	19 ± 4	10
30 s Sb_2	25%	2.9 ± 0.6	58 ± 6	19

As discussed earlier, one approach to changing from InAs to AlSb is to perform a brief growth interrupt under Sb prior to starting Al deposition. For comparison with the MEE procedure, we prepared two InAs surfaces in this way, exposing one to Sb_2 for 2 s and the other for 30 s. Images of these two surfaces are shown in Figs. 3(b) and 3(c), respectively. Although the effects of the Sb exposure are qualitatively similar in all three cases, creating vacancy islands covering about a quarter of the surface, the detailed morphology of the islands varies from case to case (Table I). Whereas the vacancy island density, area, and separation following the 30 s exposure are similar to that following MEE, the island statistics for the 2 s exposure are noticeably different. After the

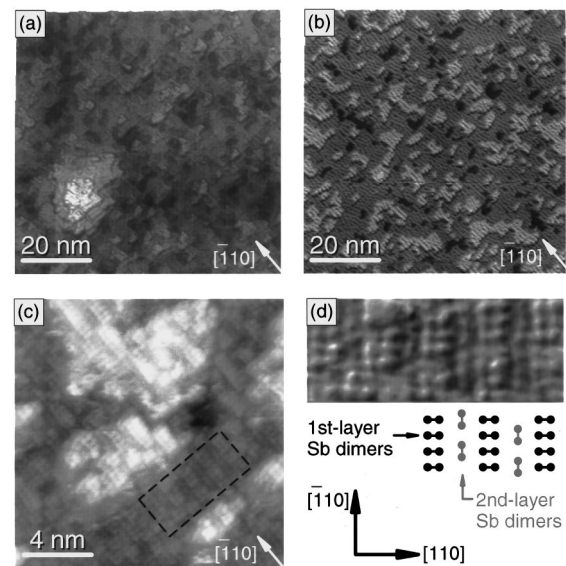


FIG. 4. Filled-state images of 5 ML of AlSb deposited on an InAs surface previously terminated with Sb via MEE [i.e., see Fig. 3(a)]. (a) Surface immediately cooled after growth (shown as a 3D-rendered gray scale, $80\ \text{nm} \times 80\ \text{nm}$). The quasi-distinct height levels occur in increments of 1–2 Å (about half the monolayer height). (b) Surface after a 5 min growth interrupt under Sb_2 (also 3D-rendered, $80\ \text{nm} \times 80\ \text{nm}$). Islands are of monolayer height, and the wavy corrugation seen on the smaller scale corresponds to the (1 \times 3)-like surface reconstruction. (c) Higher magnification view of (b), $16\ \text{nm} \times 16\ \text{nm}$, with atomic-scale features of the surface reconstruction visible. (d) Closeup of the atomically ordered region within the box in (c), gradient enhanced so that the individual atoms within the surface dimers are more easily resolved. Dimer rows separated by 13 Å are seen along the [110] direction, as are rotated dimers between the rows in the second layer. Model of the corresponding $c(2 \times 6)$ structure is shown.

shorter dose the island density is nearly an order of magnitude larger, with a much smaller distance between islands (in accord with the total island area which is constant). Dosing with Sb without the In “predose” used in MEE has another interesting effect: the resulting morphology becomes approximately isotropic between the $[1\bar{1}0]$ and $[110]$ directions. This observation suggests that the Sb adsorption/reaction is relatively isotropic, and that the anisotropy observed after MEE must therefore arise from structural anisotropy in the In prelayer. This would not be surprising given the anisotropy of the As-terminated (2×4) reconstruction.

Even these brief Sb exposures convert the InAs(001)- (2×4) reconstruction to a disordered (1×3) -like structure—characteristic of InSb—implying that Sb is rapidly incorporated into the surface. Although we expect that the MEE-prepared surface is fully Sb-terminated, at this time we have no measure of the actual Sb surface coverages. Under similar experimental conditions in a different MBE facility, the *in situ* threshold photoemission signal from InAs(001)- (2×4) changes dramatically during the first few seconds of Sb₂ exposure, and then recovers to approximately steady state after about 10 s.²⁴ Collins *et al.*²⁵ have made similar observations with RHEED. These results imply that after our 2 s exposure the surface may contain a mixture of both Sb and As. The initial signal changes observed in the photoemission and RHEED can be attributed to the disorder rapidly induced by the exchange reaction, with the more gradual recovery associated with the evolution of an Sb-terminated bilayer structure with relative atomic-scale order.

There are a number of possible causes for the bifurcation of the surface that occurs during the formation of an InSb-like interface, including strain and III/V stoichiometry changes. The 7% lattice mismatch between InSb and InAs will result in a compressively strained surface. As seen in the epitaxial growth of InSb/GaAs^{26,27} and other III–V heteroepitaxial systems, including In(Ga)As/GaAs^{28,29} and GaSb/GaAs,^{26,27,30} surface roughening acts as a strain-relief mechanism that helps lower the surface free energy. Thus, the vacancy island formation might be a similar strain-relief phenomenon. One difficulty with this mechanism is the problem with mass balance: the formation of the bilayer in this way requires long-range diffusion of atoms and/or vacancies across the large terraces, of which there is no evidence (e.g., there is no difference in the morphology near the step edges). The second possibility, a change in III/V stoichiometry, is more consistent with our results. Assuming that InAs(001)- (2×4) has the same structure as the analogous GaAs reconstruction, the top two layers of the surface are $\frac{3}{4}$ ML of In covered by $\frac{1}{2}$ ML of As.^{31–34} Converting this surface to a $c(2\times 6)$ structure composed of 1 ML of In + $\frac{2}{3}$ ML of Sb (or Sb+As) would lead to a surface deficient in In by $\frac{1}{4}$ ML, i.e., a surface with 25% vacancies. Note that such multilayer formation occurs for apparently similar reasons when Ge is deposited on GaAs(001).³⁵ This stoichiometric effect would also explain why the vacancy island coverage is independent of the way the surface is terminated

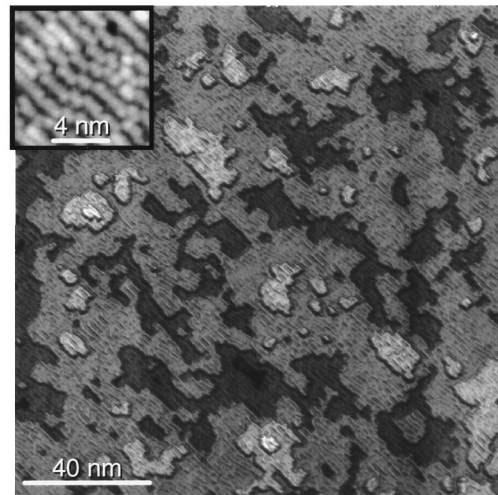


Fig. 5. 160 nm \times 160 nm 3D-rendered filled-state image of 22 ML of InAs grown on top of an interrupt-terminated AlSb layer [i.e., Fig. 4(b)]. Surface was exposed to Sb₂ for 30 s after growth. (Inset) Atomic-scale view of the (1×3) -like reconstruction observed on the surface.

with Sb. Preliminary results suggest, however, that there are growth procedures that minimize this effect, as will be discussed in detail elsewhere.³⁶

Moving beyond the formation of the InSb-like interface, we now turn our attention to the morphology of the AlSb barrier layer. Two AlSb films, each 5 ML thick, were grown on an MEE-prepared surface, with one sample immediately cooled after growth and the other given a 5 min growth interrupt under Sb₂. As observed in Fig. 4, the addition of the AlSb increases the number of layers present on the surface. Following the immediate cool-down the surface is relatively rough, with a disordered array of ~ 1 nm sized features [Fig. 4(a)]. Although the heights of the features occur mostly in increments of 1–2 Å (about half the monolayer height), the levels are not distinct enough for a histogram analysis. In contrast, after the growth interrupt the film exhibits three distinct terrace levels with (1×3) -like atomic-scale order [Figs. 4(b)–4(d)]. Statistical analysis of a number of different images of this surface shows the bottom, middle, and top layers make up 6%, 67%, and 27% of the surface, respectively. Close inspection of regions of this surface with relative atomic-scale order reveal details of the surface reconstruction. In Fig. 4(d) a gradient-enhanced image of such a region is displayed, where the individual atoms within the surface dimers are just resolved. Sb dimer rows running along the $[1\bar{1}0]$ direction are seen, as are rotated Sb dimers between the rows in the second layer, consistent with the model proposed for III-Sb(001)- $c(2\times 6)$ surfaces.^{22,23}

The final surface studied was 22 ML of InAs deposited on top of the interrupt-terminated AlSb film. To make this InAs film representative of the next interface in a double-AlSb-barrier structure, its growth was terminated by a 30 s interrupt under Sb₂. As shown in Fig. 5, this Sb-terminated InAs surface has a multilevel morphology, similar to the underlying AlSb surface. Like all the Sb-terminated surfaces, a (1×3) -like reconstruction is observed. Note that there are

TABLE II. Root-mean-square roughness determined for each of the Sb-terminated surfaces. A denotes the surface produced by MEE (alternate In and Sb₂ deposition), and B denotes the surface formed by the addition of 5 ML AlSb followed by a growth interrupt.

Sample	Figure	rms roughness (Å)
1 ML In+2 s Sb ₂ (A)	3(a)	1.1
2 s Sb ₂	3(b)	1.1
30 s Sb ₂	3(c)	1.0
A+5 ML AlSb+cool(B)	4(a)	1.5
A+5 ML AlSb+interrupt	4(b)–4(d)	1.6
B+22 ML InAs+30 s Sb ₂	5	2.0

many more kinks in the dimer rows on this surface as compared with AlSb, possibly a consequence of the shorter interrupt terminating the growth. Although the number of distinct layers increases to five, the lowest and highest levels together constitute only about 1% of the surface area. The three other levels, from lowest to highest, cover 20%, 67%, and 12% of the surface, respectively.

It is interesting that the morphology of the last InAs surface is noticeably different than that of Fig. 3(c), with island sizes approximately twice as large, even though both were exposed to Sb₂ for 30 s. A variety of factors could contribute to this difference. Because it is more practical to grow an entire structure at the same temperature, the second film was grown at a temperature ~ 100 °C lower than the buffer layer. Moreover, the second film did not benefit from the long interrupt at the higher temperature given to the buffer layer prior to Sb exposure. At the time Sb exposure begins, these two factors combined are expected to give the second surface a higher density of islands (i.e., more layers) than the nearly ideal buffer layer. Therefore, vacancies created during the short Sb dose will be able to diffuse to and incorporate into existing step edges much more readily than on the very large buffer layer terraces, suppressing the formation of additional vacancy islands.

The root-mean-square (rms) roughness determined for each of the Sb-terminated surfaces is summarized in Table II. The roughness is smallest for the initial bilayer surfaces, and increase as additional layers appear on the surface. The increase in the number of layers present on the growth front may be an indication that the temperature is too low or the growth rates are too high for step-flow. However, given the presence of strain, perfect step-flow may not be possible. Whereas a higher growth temperature and/or growth interrupts may lead to smoother interfaces, this benefit might come at the expense of additional intermixing—an effect known to be detrimental to device properties.³⁷

IV. CONCLUSIONS

We have used *in situ* STM to study the evolution of the interfaces formed during the fabrication of an InAs/AlSb/InAs RTD-like structure. InAs(001)-(2 \times 4) buffer layer surfaces were exposed to Sb₂ by several different methods to produce InSb-like bonds at the interface; all methods resulted in a bilayer surface, with vacancy islands covering

approximately 25% of the surface. In addition, all the procedures produced a (1 \times 3)-like reconstruction characteristic of an InSb-like surface terminated with >1 ML Sb, indicating that there is a significant amount of Sb on the surface. Starting with an Sb-terminated InAs surface produced by MEE (1 ML In followed by 2 s Sb₂), 5 ML AlSb and then 22 ML InAs/AlSb films were grown. The rms roughness at each subsequent interface was found to increase due to an increase in the number of distinct atomic layers present on the growth surface; however, on all the surfaces the roughness is ≤ 2 Å. The surface roughness observed is attributed to a combination of factors, including reconstruction-related stoichiometry differences, kinetically limited diffusion during growth, and lattice-mismatch strain.

Finding the optimal point in growth parameter space is a difficult task given the many variables and trade-offs involved. While we have made an initial effort to address some of these issues, it is clear that additional studies are required to isolate and ultimately identify the different factors contributing to the overall surface roughness. It is noteworthy that the interfaces in the RTD structure get rougher with each additional component layer. Thus, improving the initial Sb–InAs interface could lead to a significant reduction in the roughness of the subsequent layers. Further studies that delve into the anion exchange reactions and elucidate how the initial bilayer roughness propagates during the growth, including the effects of kinetic limitations, are required for the development of growth procedures that allow the fabrication of consistently smooth and abrupt interfaces.

ACKNOWLEDGMENTS

The authors would like to thank Dr. D. H. Chow and Dr. J. H. G. Owen for useful discussions throughout this work. This work was supported by the Office of Naval Research; QUEST, a NSF Science and Technology Center for Quantized Electronic Structures (Grant No. DMR 91-20007); DARPA/NSF, Virtual Integrated Prototyping for Epitaxial Growth, Phase I (Grant No. DMS-9615854); and the W. M. Keck Foundation (WHW).

- ¹J. S. Scott, J. P. Kaminski, S. J. Allen, D. H. Chow, M. Lui, and T. Y. Liu, *Surf. Sci.* **305**, 389 (1994).
- ²E. R. Brown, E. R. Söderström, J. R. Parker, L. J. Mahoney, K. M. Molvar, and T. C. McGill, *Appl. Phys. Lett.* **58**, 2291 (1991).
- ³J. R. Söderström, E. R. Brown, C. D. Parker, L. J. Mahoney, J. Y. Yao, T. G. Andersson, and T. C. McGill, *Appl. Phys. Lett.* **58**, 275 (1991).
- ⁴H. Kitabayashi, T. Waho, and M. Yamamoto, *Appl. Phys. Lett.* **71**, 512 (1997).
- ⁵P. Roblin, R. C. Potter, and A. Fathimulla, *J. Appl. Phys.* **79**, 2502 (1996).
- ⁶M. E. Twigg, B. R. Bennett, and B. V. Shanabrook, *Appl. Phys. Lett.* **67**, 1609 (1995).
- ⁷P. M. Thibado, B. R. Bennett, M. E. Twigg, B. V. Shanabrook, and L. J. Whitman, *Appl. Phys. Lett.* **67**, 3578 (1995).
- ⁸M. W. Wang, D. A. Collins, T. C. McGill, R. W. Grant, and R. M. Feenstra, *Appl. Phys. Lett.* **66**, 2981 (1995).
- ⁹M. W. Wang, D. A. Collins, T. C. McGill, R. W. Grant, and R. M. Feenstra, *J. Vac. Sci. Technol. B* **13**, 1689 (1995).
- ¹⁰B. R. Bennett, B. V. Shanabrook, and E. R. Glaser, *Appl. Phys. Lett.* **65**, 598 (1994).
- ¹¹K. C. Wong, C. Yang, M. Thomas, and H.-R. Blank, *J. Appl. Phys.* **82**, 4904 (1997).

- ¹²J. Schmitz, J. Wagner, F. Fuchs, N. Herres, P. Koidl, and J. D. Ralston, *J. Cryst. Growth* **150**, 858 (1994).
- ¹³B. Jenichen, H. Neuroth, B. Brar, and H. Kroemer, *Mater. Res. Soc. Symp. Proc.* **379**, 493 (1995).
- ¹⁴B. Brar, J. Ibbetson, H. Kroemer, and J. H. English, *Appl. Phys. Lett.* **64**, 3392 (1994).
- ¹⁵S.-F. Ren and J. Shen, *J. Appl. Phys.* **81**, 1169 (1997).
- ¹⁶M. W. Wang, D. A. Collins, T. C. McGill, and R. W. Grant, *J. Vac. Sci. Technol. B* **11**, 1418 (1993).
- ¹⁷L. J. Whitman, P. M. Thibado, F. Linker, and J. Patrin, *J. Vac. Sci. Technol. B* **14**, 1870 (1996).
- ¹⁸This temperature was estimated by infrared transmission measurements on an InAs film grown on a GaAs substrate. [See, for instance, B. V. Shanabrook, J. R. Waterman, J. L. Davis, and R. J. Wagner, *Appl. Phys. Lett.* **61**, 2338 (1992).] These measurements can be sensitive to the growth conditions, surface morphology, etc., and results may vary at different laboratories. For example, a similar experiment in a different lab determined the transition temperature to be ~ 40 °C higher than we observed.
- ¹⁹C. F. McConville, T. S. Jones, F. M. Leibsle, S. M. Driver, T. C. Q. Noakes, M. O. Schweitzer, and N. V. Richardson, *Phys. Rev. B* **50**, 14965 (1994).
- ²⁰P. M. Thibado, B. R. Bennett, B. V. Shanabrook, and L. J. Whitman, *J. Cryst. Growth* **175/176**, 317 (1997).
- ²¹G. E. Franklin, D. H. Rich, A. Samsavar, E. S. Hirschorn, F. M. Leibsle, T. Miller, and T.-C. Chiang, *Phys. Rev. B* **41**, 12619 (1990).
- ²²U. Resch-Esser, N. Esser, B. Brar, and H. Kroemer, *Phys. Rev. B* **55**, 15401 (1997).
- ²³M. T. Sieger, T. Miller, and T.-C. Chiang, *Phys. Rev. B* **52**, 8256 (1995).
- ²⁴J. J. Zinck (to be published).
- ²⁵D. A. Collins, M. W. Wang, R. W. Grant, and T. C. McGill, *J. Vac. Sci. Technol. B* **12**, 1125 (1994).
- ²⁶B. R. Bennett, P. M. Thibado, M. E. Twigg, E. R. Glaser, R. Magno, B. V. Shanabrook, and L. J. Whitman, *J. Vac. Sci. Technol. B* **14**, 2195 (1996).
- ²⁷B. R. Bennett, B. V. Shanabrook, P. M. Thibado, L. J. Whitman, and R. Magno, *J. Cryst. Growth* **175/176**, 888 (1997).
- ²⁸D. Leonard, M. Krishnamurthy, C. M. Reaves, S. P. DenBaars, and P. M. Petroff, *Appl. Phys. Lett.* **63**, 3203 (1993).
- ²⁹V. Bressler-Hill, S. Varma, A. Lorke, B. Z. Nosho, P. M. Petroff, and W. H. Weinberg, *Phys. Rev. Lett.* **74**, 3209 (1995).
- ³⁰P. M. Thibado, B. R. Bennett, M. E. Twigg, B. V. Shanabrook, and L. J. Whitman, *J. Vac. Sci. Technol. A* **14**, 885 (1996).
- ³¹D. J. Chadi, *J. Vac. Sci. Technol. A* **5**, 834 (1987).
- ³²Q. K. Xue, T. Hashizume, T. Sakata, and Y. Hasegawa, *Thin Solid Films* **281–282**, 556 (1996).
- ³³A. R. Avery, C. M. Goringe, D. M. Holmes, J. L. Sudijono, and T. S. Jones, *Phys. Rev. Lett.* **76**, 3344 (1996).
- ³⁴C. B. Duke, *Surf. Sci.* **65**, 543 (1993).
- ³⁵X. S. Wang, K. Self, D. Leonard, V. Bressler-Hill, R. Maboudian, W. H. Petroff, and W. H. Weinberg, *J. Vac. Sci. Technol. B* **11**, 1477 (1993).
- ³⁶B. Z. Nosho, B. V. Shanabrook, B. R. Bennett, W. H. Weinberg, J. J. Zinck, and L. J. Whitman (to be published).
- ³⁷M. J. Yang, W. J. Moore, B. R. Bennett, and B. V. Shanabrook, *Electron. Lett.* **34**, 270 (1998).